

Accelerated Sequential Posterior Inference via Reuse for Gravitational-Wave Analyses

Michael J. Williams *

Institute of Cosmology and Gravitation, University of Portsmouth, Portsmouth PO1 3FX, United Kingdom

(Dated: November 7, 2025)

We introduce Accelerated Sequential Posterior Inference via Reuse (ASPIRE), a broadly applicable framework that transforms existing posterior samples and Bayesian evidence estimates into unbiased results under alternative models without rerunning the original analysis. ASPIRE combines normalizing flows with a generalized Sequential Monte Carlo scheme, enabling efficient updates of existing results and reducing the computational cost of reanalyses by 4–10 times. This addresses a growing problem in gravitational-wave astronomy, where events must be repeatedly reanalyzed under different models or physical hypotheses. We show that ASPIRE reproduces full Bayesian results when switching waveform models or adding physical effects such as spin precession and orbital eccentricity. With this statistical robustness, ASPIRE turns repeated reanalyses into fast, reliable updates—paving the way for systematic studies of waveform systematics, scalable reanalyses across large event catalogs, and broadly applicable Bayesian reanalysis across other scientific domains.

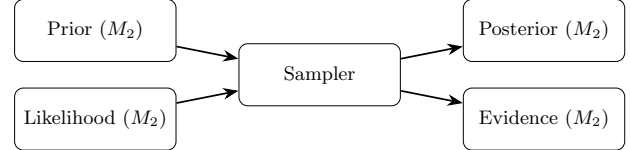
Introduction—The LIGO-Virgo-KAGRA collaboration [1–3] has detected more than 200 gravitational-wave signals from compact binary mergers [4–8] and continues to regularly detect such signals [9]. These detections have shaped our understanding of the Universe on multiple scales [10] and allowed us to probe the validity of General Relativity [11]. As the catalog of events grows, a key challenge emerges: events must be reanalyzed repeatedly under different models or physical hypotheses. Understanding waveform systematics [12, 13], adding effects such as orbital eccentricity [14, 15], performing tests of General Relativity [16], or modeling gravitational-lensing [17] all require new analyses from scratch. This repeated reanalysis is rapidly becoming a computational bottleneck, limiting our ability to probe waveform systematics and to conduct comprehensive tests of fundamental physics.

Ideally, existing results would inform subsequent analyses. Naively using an earlier posterior as the prior for a new analysis breaks model comparison, since priors must remain consistent across models. Instead, one must look to an algorithm that can incorporate existing samples and still produce unbiased estimates of the posterior distribution and Bayesian evidence. Current analyses typically use nested sampling [18, 19] which produces robust estimates of both the posterior and evidence but can take hours to days [20, 21]. Many efforts have sought to accelerate inference [22–27], yet these require analyses to restart from the prior when changing the model, fail when the initial and target posteriors occupy different regions of parameter space or do not provide robust evidence estimates at comparable cost [28–31].

Here we present a novel framework: Accelerated Sequential Posterior Inference via Reuse (ASPIRE). Instead of discarding existing results and repeating full analyses, posterior samples and the evidence estimate obtained under one model are updated to unbiased posterior samples and an evidence estimate under a new model. This approach remains valid even when the two posteriors occupy different regions of parameter space or

Starting point: Posterior Samples (M_1), New Model (M_2)

Traditional inference



ASPIRE

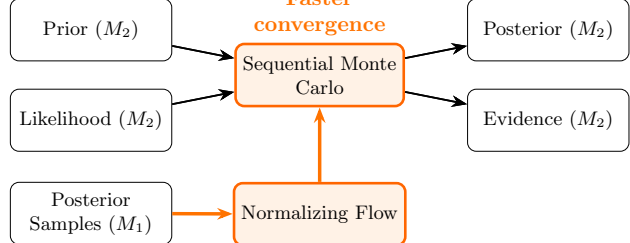


FIG. 1. Comparison of traditional Bayesian inference (top), which must perform full inference for a new model M_2 despite existing posterior samples with M_1 , with ASPIRE (bottom), which reuses the existing posterior samples under model M_1 via flow approximation and an SMC update to obtain unbiased results under a new model M_2 .

when new parameters must be introduced, making it possible to extend existing analyses to include additional physical effects, such as extending existing results to include the effects of orbital eccentricity [32], or to confront entire families of modified-gravity hypotheses with data [16]. ASPIRE thus enables repeated reanalyses via sequential reuse of existing results.

ASPIRE combines normalizing flows with a generalized SMC scheme. We show that ASPIRE is robust and reproduces results that are statistically identical to a traditional analysis while reducing computational cost by 4–10 times. We demonstrate efficient updates between different waveform models, recovery of new pa-

rameters such as for modelling spin precession [33] and orbital eccentricity [32], and highlight an application to real data. By enabling analyses to be updated rather than repeated, ASPIRE provides a broadly applicable tool for gravitational-wave astronomy and other areas of physics where reanalyses are common.

Method—Bayesian inference traditionally proceeds by assuming a model M_1 that describes the data d and has parameters θ . It then combines a prior $p(\theta|M_1)$ with a likelihood $p(d|\theta, M_1)$ to obtain a posterior distribution $p(\theta|M_1, d)$. Each time the underlying model or data changes, the full inference must be repeated from scratch, discarding all previous results (fig. 1, top). This repeated reanalysis is costly and increasingly impractical as data volumes and model complexities grow.

The ASPIRE framework introduces a new approach to sequentially updating existing results and requires two complementary steps. Instead of restarting from draws from the prior, ASPIRE begins with posterior samples obtained under an existing model M_1 (fig. 1, bottom left). We approximate these samples using a normalizing flow [34], a flexible density estimator that maps a simple base distribution $q_z(z)$ into an approximation of the posterior $q_\phi(\theta)$ through an invertible transformation $f_\phi(\theta)$ described by parameters ϕ . Training the flow on the initial samples by maximum likelihood [34] yields

$$p(\theta|d, M_1) \approx q_\phi(\theta) = q_z(f_\phi(\theta)) \left| \frac{\partial f_\phi(\theta)}{\partial \theta} \right|, \quad (1)$$

from which we can both generate new samples and evaluate densities across parameter space. This allows ASPIRE to start from an informed initial distribution rather than the prior. When the target model M_2 has different parameters, we extend the initial samples by drawing new parameters from the prior and discarding incompatible ones, ensuring that q_ϕ spans the space of M_2 (see the Supplemental Material [35] for more details).

The second step (fig. 1, bottom middle) is to evolve this distribution into the target posterior and to estimate the Bayesian evidence. We build on [36] and generalize SMC for this purpose. SMC for Bayesian inference evolves a set of samples through a sequence of intermediate distributions that interpolate between the prior and posterior via an inverse temperature β_t that anneals the likelihood [37]. In ASPIRE, the sequence instead interpolates between the flow-based approximation $q_\phi(\theta)$ and the true posterior under the new model M_2 :

$$p_t(\theta|d, M_2, \beta_t) \propto q_\phi(\theta)^{1-\beta_t} [p(d|\theta, M_2)p(\theta|M_2)]^{\beta_t}, \quad (2)$$

where $\beta_t \in [0, 1]$ controls the progression. The algorithm starts with samples from q_ϕ and then at each iteration i , the inverse temperature β_i is increased using an adaptive schedule. The samples are resampled according to $p_i(\theta|d, M_2, \beta_i)/p_{i-1}(\theta|d, M_2, \beta_{i-1})$ and then diversified using an Markov Chain Monte Carlo (MCMC)

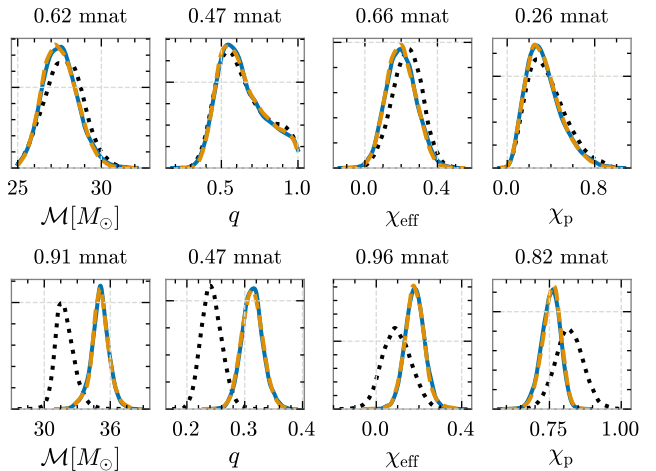


FIG. 2. Posterior samples obtained from analyzing two simulated signals with different waveform models. **Top:** GW150914-like system with comparable masses and low spins. **Bottom:** highly spinning asymmetric system with $m_1/m_2 = 4$. Results are shown for IMRPhenomXPHM using standard sampling with *dynesty* (black dotted line), IMRPhenomX04a using ASPIRE, initialized from the IMRPhenomXPHM samples (orange dashed line) and IMRPhenomX04a using standard sampling with *dynesty* (blue solid line). Parameters shown are chirp mass, mass ratio, effective aligned spin χ_{eff} and effective precessing spin χ_p . The JSR in millinats (mnats) between the two IMRPhenomX04a posteriors is quoted above each subplot and show that the results are consistent.

step [38, 39]. The algorithm terminates when $\beta_t = 1$, producing posterior samples and an evidence estimate. This approach guarantees unbiased results, even when the target and initial posteriors occupy different regions of the parameter space.

Together, these two components, flow-based posterior approximation and generalized SMC evolution, define ASPIRE. This enables efficient reuse of existing results and allows analyses to be updated rather than repeated. The implementation details are provided in the Supplemental Material [35] and we provide an open-source implementation in the Python package `aspire` [40].

Results—We evaluate ASPIRE across simulated and real data, testing its robustness to waveform choice, added physical complexity, and detector calibration uncertainties.

We assess ASPIRE when changing the waveform model used to describe the signal, a key test for evaluating systematic uncertainties. We consider two waveform models that include spin precession and higher-order multipoles: IMRPhenomXPHM [41] and IMRPhenomX04a [42], both used in GWTC-4.0 [8] for understanding waveform systematics. Figure 2 compares results for two simulated signals analyzed with both waveforms, where ASPIRE updates an initial IMRPhenomXPHM run to obtain results consistent with IMRPhenomX04a. We quantify the similarity be-

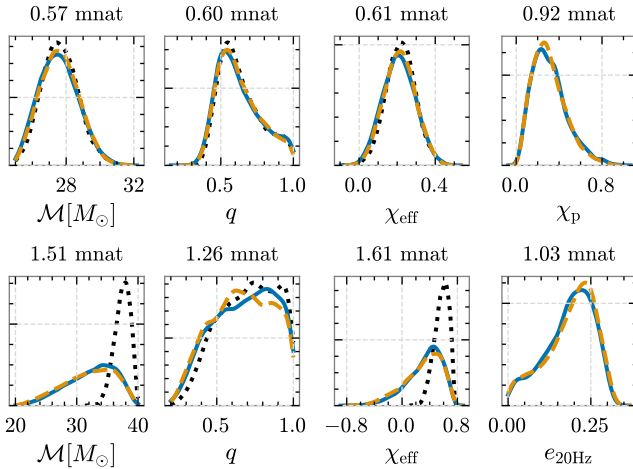


FIG. 3. Posterior samples obtained when adding new physics to an initial analysis. **Top:** spin-precessing analysis of a GW150914 injection, results are shown for the Gray: **IMRPhenomD** (aligned spins) baseline with **dynesty** (black dotted line), **IMRPhenomPv2** (precessing spins) using **ASPIRE** initialized from the aligned-spin samples (orange dashed-line) and an **IMRPhenomPv2** using standard sampling with **dynesty** (blue solid line). **Bottom:** eccentric analysis of an aligned-spin GW150914 injection, results are shown for the **TaylorF2** baseline with **dynesty** (black dotted line), **TaylorF2Ecc** using **ASPIRE** initialized from the **TaylorF2** result (orange dashed line) and **TaylorF2Ecc** using standard sampling with **dynesty** (blue solid line). Parameters shown are chirp mass, mass ratio, effective aligned spin χ_{eff} , and effective precessing spin χ_p (top row) or eccentricity at 20 Hz $e_{20\text{Hz}}$ (bottom row). The JSD in millinats (mnats) between the posteriors with same waveform is quoted above each subplot and demonstrate consistency.

tween posterior distributions using the JSD (D_{JS}) in millinats (mnats), where larger values indicate greater differences and $D_{\text{JS}} \leq 1.5$ mnats denotes good agreement [21]. For both systems, the posteriors obtained with ASPIRE are in close agreement with the baseline ($D_{\text{JS}} < 1.5$ mnats), even for the asymmetric binary where the posterior shifts substantially. In terms of computational cost, analyses with ASPIRE require 7 and 6 times fewer likelihood evaluations per sample for the GW150914-like and asymmetric injections, respectively, corresponding to a reduction in the time per sample by factors of 6 and 5.

We extend the analyses to models that incorporate additional physics, namely spin precession and orbital eccentricity.

Starting with spin precession, we use ASPIRE to update a result originally obtained under the aligned-spin assumption with **IMRPhenomD** [43, 44], replacing it with the precessing model **IMRPhenomPv2** [45, 46]. This type of update is particularly relevant in low-latency analyses, where simplifying assumptions are often made to reduce computational cost [47]. In fig. 3 (top), we compare the posterior distributions and find that ASPIRE remains

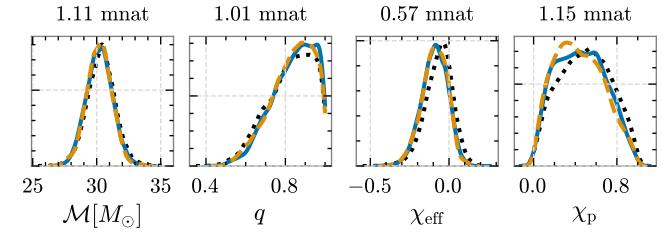


FIG. 4. Posterior distributions for GW150914 with chirp mass and mass ratio and aligned spin χ_{eff} and effective precessing spin χ_p . Results are shown for an initial analysis with **IMRPhenomXPHM** and **dynesty** (black dotted line), an analysis with **IMRPhenomX04a** and **ASPIRE**, updated from the initial analysis (orange dashed line) and a baseline analysis **IMRPhenomX04a** and **dynesty** (blue solid line). The JSD in millinats (mnats) between the posteriors with same waveform is quoted above each subplot and confirm that the results are consistent.

consistent with a baseline analysis with $D_{\text{JS}} < 1.5$ mnats. This includes the precessing-spin parameter χ_p , which captures physical effects absent from the initial aligned-spin analysis. Notably, ASPIRE achieves this while reducing the number of evaluations and time per sample by 10 times.

Orbital eccentricity has become an increasingly important focus within gravitational-wave astronomy, as it provides a clear signature of dynamical formation channels [48] and several observed events show potential evidence for it [49–52]. However, incorporating eccentricity typically requires reanalyzing existing events, which can be computationally expensive. To demonstrate the robustness of this approach using a simulated signal with an eccentricity at 20 Hz of 0.25, we show how ASPIRE can extend a result obtained under the quasi-circular, aligned-spin assumption with **TaylorF2** [53], updating it with the eccentric waveform model **TaylorF2Ecc** [54]. In fig. 3 (bottom), we present the posterior distributions, including the eccentricity posterior, which agrees with the baseline analysis. The distributions show good agreement, while ASPIRE achieves a 7-fold reduction in evaluations per sample corresponding to a 6 times improvement in the time per sample.

These examples illustrate that ASPIRE correctly incorporates new physical degrees of freedom without introducing bias, even in cases where the added parameters are strongly correlated with existing ones.

We demonstrate that ASPIRE can be applied to real data by reanalyzing the first detection, GW150914 [55], incorporating the 40 additional parameters required to model the uncertain calibration of the detectors [56]. We replicate a typical catalog analysis [57]: first analyzing GW150914 with **IMRPhenomXPHM**, and then using ASPIRE to obtain results with **IMRPhenomX04a**. GW150914 lies in a region of parameter space where these two waveform models are expected to broadly agree. In fig. 4, we

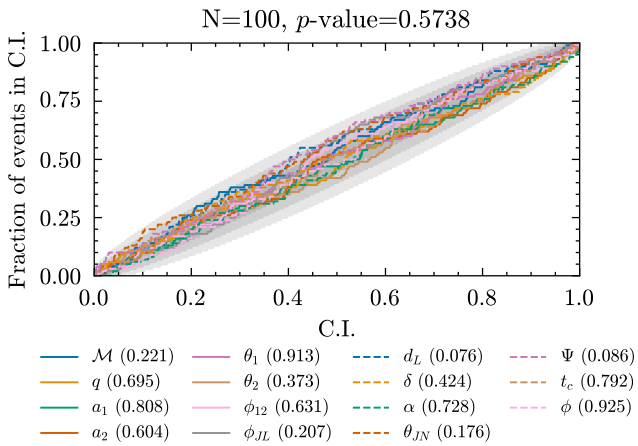


FIG. 5. Probability–probability (P–P) plot for 100 simulated binary black hole signals analyzed with ASPIRE. Signals were generated with `IMRPhenomXPHM` in a three-detector network and analyzed using `bilby` with `dynesty`. Initial samples were drawn from the prior to initialize ASPIRE. Shaded regions indicate 1-, 2-, and 3- σ confidence intervals. The combined p -value of 0.574 demonstrates that the posteriors are statistically unbiased.

show the posterior distributions for the masses and spins, which differ slightly, consistent with similar reanalyses of this event [58, 59]. The results obtained with ASPIRE are fully consistent with a baseline analysis, while requiring 4 times fewer likelihood evaluations per sample, which corresponds to a 7-fold reduction in time per sample. This demonstrates that ASPIRE handles the additional challenges of analyzing real data while retaining its efficiency.

To further demonstrate that ASPIRE produces statistically unbiased posterior distributions, we perform a probability–probability (P–P) test with 100 simulated binary black hole signals with spin-precession and higher-order multipoles. We analyze these signals with ASPIRE and use initial samples from the prior. This produces the P–P plot shown in fig. 5 with combined p -value of 0.574, confirming that the inferred posteriors are unbiased.

In addition to recovering unbiased posterior distributions, ASPIRE yields consistent evidence estimates which distinguishes it from other methods such as MCMC. In table I we present the inferred log-evidences for analyses using ASPIRE and `dynesty` with the same waveform. The log-evidence differences between ASPIRE and `dynesty` are within the estimated uncertainties, except for the asymmetric injection where they differ slightly. This serves as additional confirmation that the results obtained with ASPIRE are consistent with traditional approaches and that ASPIRE maintains statistical validity for model comparison.

Discussion and outlook—ASPIRE establishes a novel approach for Bayesian inference in gravitational-wave as-

tronomy. Rather than discarding results and restarting analyses from the prior, posterior results can be transformed into unbiased results under new models, including new posterior samples and an evidence estimate, that are consistent with traditional analyses. This capability goes beyond existing acceleration methods, which either fail when posteriors occupy different regions of parameter space, lack robust evidence estimates at comparable cost, or still require costly full reanalyses [22–31]. By demonstrating that sequential inference via reuse of existing results is both practical and statistically robust, ASPIRE provides a new tool for systematic exploration of waveform systematics and physical hypotheses.

Our studies highlight the immediate utility of this approach. ASPIRE reproduces full Bayesian results across waveform approximants, recovers additional physical effects such as spin precession and orbital eccentricity, and passes stringent statistical validation tests. In all cases, the method yields posteriors and evidence estimates consistent with baseline inferences while reducing computational costs by 4–10 times. These gains transform tasks that were previously prohibitive, such as repeated waveform comparisons or large-scale catalog updates, into routine analyses. In doing so, ASPIRE maximizes the scientific return from the rapidly growing catalog of gravitational-wave detections [8].

Looking forward, the framework offers clear paths for further improvement. Enhanced SMC methods, including gradient-based proposals [60] and recycling of particles across iterations [61, 62] could provide order-of-magnitude accelerations beyond those reported here. Since SMC is naturally parallelizable, ASPIRE is well suited to GPUs and high-performance computing environments, and can be adapted for real-time or low-latency applications. Furthermore, one could explore alternative methods to SMC such as other tempered MCMC approaches [30, 63]. These developments position ASPIRE to benefit directly from advances in both algorithms and computing hardware.

Beyond methodological advances, ASPIRE has a wide range of potential applications. In gravitational-wave astronomy, it can support systematic waveform-model comparisons, large-scale tests of General Relativity, rapid reanalyses of candidate events, and efficient updates of entire catalogs as models improve. It could be used to refine approximate posterior estimates from low-latency approaches [26, 27, 64]. Early-warning and low-latency pipelines [47, 65] could incorporate ASPIRE to refine source characterization in real time. The framework also extends naturally to other fields where competing models abound, such as reinterpreting particle physics measurements under alternative theoretical models [66] or reanalysing cosmological data when performing Bayesian model comparison [67, 68]. By enabling fast and unbiased reanalyses, ASPIRE opens the way to scalable and systematic Bayesian inference across diverse scientific do-

TABLE I. Estimated log-Bayesian evidences (base e) for the five comparisons performed using ASPIRE and the baseline, `dynesty`.

Analysis	Waveform	<code>aspire</code>	<code>dynesty</code>
Changing waveform (GW150914-like)	<code>IMRPhenomX04a</code>	-57893.36 +/- 0.06	-57893.23 +/- 0.16
Changing waveform ($q = 4$)	<code>IMRPhenomX04a</code>	-54803.08 +/- 0.09	-54802.73 +/- 0.21
Adding spin precession	<code>IMRPhenomPv2</code>	-57893.10 +/- 0.06	-57893.12 +/- 0.15
Adding orbital eccentricity	<code>TaylorF2Ecc</code>	-1928.21 +/- 0.08	-1928.15 +/- 0.16
GW150914 (real data)	<code>IMRPhenomX04a</code>	-12768.08 +/- 0.07	-12767.84 +/- 0.16

mains.

Acknowledgments—The author thanks Colm Talbot and Konstantin Leyde for insightful discussions and Ian Harry and Chris Messenger for feedback on the manuscript. This work benefited from discussions at AIIslands 2025: Bute, on 13 to 15 May, 2025 and EuCAIFCon 2025, 16 to 20 June, 2025. The author thanks the organizers and participants for their feedback and insights. MJW acknowledges support from ST/X002225/1, ST/Y004876/1 and the University of Portsmouth. The author is grateful for computational resources provided by the LIGO Laboratory and Cardiff University and supported by National Science Foundation Grants PHY-0757058 and PHY-0823459 and STFC grants ST/I006285/1 and ST/V005618/1. Additional numerical computations were carried out on the SCIMMA High Performance Compute (HPC) cluster which is supported by the ICG and the University of Portsmouth. This material is based upon work supported by NSF’s LIGO Laboratory which is a major facility fully funded by the National Science Foundation. The author acknowledges the use of ChatGPT (GPT-4-turbo and GPT-5) for proofreading and polishing the manuscript; all AI-generated text was carefully reviewed and edited by the author to ensure accuracy.

Data availability—The results presented in this letter and code to reproduce the analyses are available at [69, 70]. The `aspire`, `aspire-bilby` and `aspire-gw` software packages are available via PyPI [71–73] and the source code at <https://github.com/mj-will/aspire>, <https://github.com/mj-will/aspire-bilby> and <https://github.com/mj-will/aspire-gw>. Interferometric data for GW150914 is provided by the LIGO-Virgo-KAGRA Collaboration via GWOSC [74].

Software—This used the following software packages: `array-api-compat` [75], `bilby` [76, 77], `bilby_pipe` [21], `corner` [78], `dynesty` [79], `gwflow` [80], `LALSuite` [81, 82], `matplotlib` [83], `minipcn` [84], `numpy` [85], `PESummary` [86], `PyTorch` [87], `scipy` [88, 89], `seaborn` [90], `zuko` [91].

Quant. **Grav.** **32**, 074001 (2015), arXiv:1411.4547 [gr-qc].

- [2] F. Acernese *et al.* (VIRGO), Advanced Virgo: a second-generation interferometric gravitational wave detector, *Class. Quant. Grav.* **32**, 024001 (2015), arXiv:1408.3978 [gr-qc].
- [3] T. Akutsu *et al.* (KAGRA), Overview of KAGRA: Detector design and construction history, *PTEP* **2021**, 05A101 (2021), arXiv:2005.05574 [physics.ins-det].
- [4] B. P. Abbott *et al.* (LIGO Scientific, Virgo), GWTC-1: A Gravitational-Wave Transient Catalog of Compact Binary Mergers Observed by LIGO and Virgo during the First and Second Observing Runs, *Phys. Rev. X* **9**, 031040 (2019), arXiv:1811.12907 [astro-ph.HE].
- [5] R. Abbott *et al.* (LIGO Scientific, Virgo), GWTC-2: Compact Binary Coalescences Observed by LIGO and Virgo During the First Half of the Third Observing Run, *Phys. Rev. X* **11**, 021053 (2021), arXiv:2010.14527 [gr-qc].
- [6] R. Abbott *et al.* (LIGO Scientific, VIRGO), GWTC-2.1: Deep extended catalog of compact binary coalescences observed by LIGO and Virgo during the first half of the third observing run, *Phys. Rev. D* **109**, 022001 (2024), arXiv:2108.01045 [gr-qc].
- [7] R. Abbott *et al.* (KAGRA, VIRGO, LIGO Scientific), GWTC-3: Compact Binary Coalescences Observed by LIGO and Virgo during the Second Part of the Third Observing Run, *Phys. Rev. X* **13**, 041039 (2023), arXiv:2111.03606 [gr-qc].
- [8] GWTC-4.0: Updating the Gravitational-Wave Transient Catalog with Observations from the First Part of the Fourth LIGO-Virgo-KAGRA Observing Run (2025), arXiv:2508.18082 [gr-qc].
- [9] L. S. Collaboration, LIGO-G2302098: LIGO-Virgo-KAGRA Cumulative Detection plot - O1-O4b, <https://dcc.ligo.org/LIGO-G2302098-v15/public> (2025), accessed: July 7, 2025.
- [10] R. Abbott *et al.* (LIGO Scientific, Virgo, KAGRA), Constraints on the Cosmic Expansion History from GWTC-3, *Astrophys. J.* **949**, 76 (2023), arXiv:2111.03604 [astro-ph.CO].
- [11] GWTC-4.0: Constraints on the Cosmic Expansion Rate and Modified Gravitational-wave Propagation (2025), arXiv:2509.04348 [astro-ph.CO].
- [12] R. Gamba, M. Breschi, S. Bernuzzi, M. Agathos, and A. Nagar, Waveform systematics in the gravitational-wave inference of tidal parameters and equation of state from binary neutron star signals, *Phys. Rev. D* **103**, 124015 (2021), arXiv:2009.08467 [gr-qc].
- [13] A. B. Yelikar, R. O. Shaughnessy, J. Lange, and A. Z. Jan, Waveform systematics in gravitational-wave inference of signals from binary neutron star merger mod-

* michael.williams3@port.ac.uk

[1] J. Aasi *et al.* (LIGO Scientific), Advanced LIGO, *Class.*

els incorporating higher-order modes information, *Phys. Rev. D* **110**, 064024 (2024), arXiv:2404.16599 [gr-qc].

[14] A. Gamboa *et al.*, Accurate waveforms for eccentric, aligned-spin binary black holes: The multipolar effective-one-body model SEOBNRv5EHM (2024), arXiv:2412.12823 [gr-qc].

[15] A. Nagar, R. Gamba, P. Rettegno, V. Fantini, and S. Bernuzzi, Effective-one-body waveform model for non-circularized, planar, coalescing black hole binaries: The importance of radiation reaction, *Phys. Rev. D* **110**, 084001 (2024), arXiv:2404.05288 [gr-qc].

[16] N. V. Krishnendu and F. Ohme, Testing General Relativity with Gravitational Waves: An Overview, *Universe* **7**, 497 (2021), arXiv:2201.05418 [gr-qc].

[17] R. Abbott *et al.* (LIGO Scientific, VIRGO), Search for Lensing Signatures in the Gravitational-Wave Observations from the First Half of LIGO–Virgo’s Third Observing Run, *Astrophys. J.* **923**, 14 (2021), arXiv:2105.06384 [gr-qc].

[18] J. Skilling, Nested Sampling, *AIP Conf. Proc.* **735**, 395 (2004).

[19] J. Skilling, Nested sampling for general Bayesian computation, *Bayesian Analysis* **1**, 833 (2006).

[20] J. Veitch *et al.*, Parameter estimation for compact binaries with ground-based gravitational-wave observations using the LALInference software library, *Phys. Rev. D* **91**, 042003 (2015), arXiv:1409.7215 [gr-qc].

[21] I. M. Romero-Shaw *et al.*, Bayesian inference for compact binary coalescences with bilby: validation and application to the first LIGO–Virgo gravitational-wave transient catalogue, *Mon. Not. Roy. Astron. Soc.* **499**, 3295 (2020), arXiv:2006.00714 [astro-ph.IM].

[22] M. J. Williams, J. Veitch, and C. Messenger, Nested sampling with normalizing flows for gravitational-wave inference, *Phys. Rev. D* **103**, 103006 (2021), arXiv:2102.11056 [gr-qc].

[23] M. J. Williams, J. Veitch, and C. Messenger, Importance nested sampling with normalising flows, *Mach. Learn. Sci. Tech.* **4**, 035011 (2023), arXiv:2302.08526 [astro-ph.IM].

[24] A. J. K. Chua and M. Vallisneri, Learning Bayesian posteriors with neural networks for gravitational-wave inference, *Phys. Rev. Lett.* **124**, 041102 (2020), arXiv:1909.05966 [gr-qc].

[25] H. Gabbard, C. Messenger, I. S. Heng, F. Tonolini, and R. Murray-Smith, Bayesian parameter estimation using conditional variational autoencoders for gravitational-wave astronomy, *Nature Phys.* **18**, 112 (2022), arXiv:1909.06296 [astro-ph.IM].

[26] M. Dax, S. R. Green, J. Gair, M. Pürer, J. Wildberger, J. H. Macke, A. Buonanno, and B. Schölkopf, Neural Importance Sampling for Rapid and Reliable Gravitational-Wave Inference, *Phys. Rev. Lett.* **130**, 171403 (2023), arXiv:2210.05686 [gr-qc].

[27] S. Fairhurst, C. Hoy, R. Green, C. Mills, and S. A. Usman, Simple parameter estimation using observable features of gravitational-wave signals, *Phys. Rev. D* **108**, 082006 (2023), arXiv:2304.03731 [gr-qc].

[28] D. W. Hogg and D. Foreman-Mackey, Data analysis recipes: Using Markov Chain Monte Carlo, *Astrophys. J. Suppl.* **236**, 11 (2018), arXiv:1710.06068 [astro-ph.IM].

[29] J. Lange, R. O’Shaughnessy, and M. Rizzo, Rapid and accurate parameter inference for coalescing, precessing compact binaries (2018), arXiv:1805.10457 [gr-qc].

[30] N. E. Wolfe, C. Talbot, and J. Golomb, Accelerating tests of general relativity with gravitational-wave signals using hybrid sampling, *Phys. Rev. D* **107**, 104056 (2023), arXiv:2208.12872 [gr-qc].

[31] M. Prathaban, H. Bevins, and W. Handley, Accelerated nested sampling with β -flows for gravitational waves (2024), arXiv:2411.17663 [astro-ph.IM].

[32] P. C. Peters and J. Mathews, Gravitational radiation from point masses in a Keplerian orbit, *Phys. Rev.* **131**, 435 (1963).

[33] T. A. Apostolatos, C. Cutler, G. J. Sussman, and K. S. Thorne, Spin induced orbital precession and its modulation of the gravitational wave forms from merging binaries, *Phys. Rev. D* **49**, 6274 (1994).

[34] G. Papamakarios, E. Nalisnick, D. J. Rezende, S. Mohamed, and B. Lakshminarayanan, Normalizing Flows for Probabilistic Modeling and Inference, *J. Machine Learning Res.* **22**, 2617 (2021), arXiv:1912.02762 [stat.ML].

[35] See Supplemental Material at [URL will be inserted by publisher] for additional figures, derivations, and experimental details.

[36] M. J. Williams, M. Karamanis, Y. Luo, and U. Seljak, Validating Sequential Monte Carlo for Gravitational-Wave Inference (2025), arXiv:2506.18977 [astro-ph.IM].

[37] J. Bernardo, M. Bayarri, J. Berger, A. Dawid, D. Heckerman, A. Smith, M. West, P. Del Moral, A. Doucet, and A. Jasra, Sequential monte carlo for bayesian computation, *Bayesian statistics* **8**, 1 (2011).

[38] P. Del Moral, A. Doucet, and A. Jasra, An adaptive sequential monte carlo method for approximate bayesian computation, *Statistics and computing* **22**, 1009 (2012).

[39] P. Fearnhead and B. M. Taylor, An Adaptive Sequential Monte Carlo Sampler, *Bayesian Analysis* **8**, 411 (2013).

[40] M. J. Williams and KonstantinLeyde, [mj-will/aspire: v0.1.0a2](https://mj-will/aspire/v0.1.0a2) (2025).

[41] G. Pratten *et al.*, Computationally efficient models for the dominant and subdominant harmonic modes of precessing binary black holes, *Phys. Rev. D* **103**, 104056 (2021), arXiv:2004.06503 [gr-qc].

[42] J. E. Thompson, E. Hamilton, L. London, S. Ghosh, P. Kolitsidou, C. Hoy, and M. Hannam, PhenomXO4a: a phenomenological gravitational-wave model for precessing black-hole binaries with higher multipoles and asymmetries, *Phys. Rev. D* **109**, 063012 (2024), arXiv:2312.10025 [gr-qc].

[43] S. Husa, S. Khan, M. Hannam, M. Pürer, F. Ohme, X. Jiménez Forteza, and A. Bohé, Frequency-domain gravitational waves from nonprecessing black-hole binaries. I. New numerical waveforms and anatomy of the signal, *Phys. Rev. D* **93**, 044006 (2016), arXiv:1508.07250 [gr-qc].

[44] S. Khan, S. Husa, M. Hannam, F. Ohme, M. Pürer, X. Jiménez Forteza, and A. Bohé, Frequency-domain gravitational waves from nonprecessing black-hole binaries. II. A phenomenological model for the advanced detector era, *Phys. Rev. D* **93**, 044007 (2016), arXiv:1508.07253 [gr-qc].

[45] P. Schmidt, M. Hannam, and S. Husa, Towards models of gravitational waveforms from generic binaries: A simple approximate mapping between precessing and non-precessing inspiral signals, *Phys. Rev. D* **86**, 104063 (2012), arXiv:1207.3088 [gr-qc].

[46] M. Hannam, P. Schmidt, A. Bohé, L. Haegel, S. Husa,

F. Ohme, G. Pratten, and M. Pürer, Simple Model of Complete Precessing Black-Hole-Binary Gravitational Waveforms, *Phys. Rev. Lett.* **113**, 151101 (2014), [arXiv:1308.3271 \[gr-qc\]](https://arxiv.org/abs/1308.3271).

[47] S. Morisaki, R. Smith, L. Tsukada, S. Sachdev, S. Stevenson, C. Talbot, and A. Zimmerman, Rapid localization and inference on compact binary coalescences with the Advanced LIGO-Virgo-KAGRA gravitational-wave detector network, *Phys. Rev. D* **108**, 123040 (2023), [arXiv:2307.13380 \[gr-qc\]](https://arxiv.org/abs/2307.13380).

[48] I. Mandel and F. S. Broekgaarden, Rates of compact object coalescences, *Living Rev. Rel.* **25**, 1 (2022), [arXiv:2107.14239 \[astro-ph.HE\]](https://arxiv.org/abs/2107.14239).

[49] I. M. Romero-Shaw, P. D. Lasky, E. Thrane, and J. C. Bustillo, GW190521: orbital eccentricity and signatures of dynamical formation in a binary black hole merger signal, *Astrophys. J. Lett.* **903**, L5 (2020), [arXiv:2009.04771 \[astro-ph.HE\]](https://arxiv.org/abs/2009.04771).

[50] I. M. Romero-Shaw, P. D. Lasky, and E. Thrane, Four Eccentric Mergers Increase the Evidence that LIGO-Virgo-KAGRA's Binary Black Holes Form Dynamically, *Astrophys. J.* **940**, 171 (2022), [arXiv:2206.14695 \[astro-ph.HE\]](https://arxiv.org/abs/2206.14695).

[51] N. Gupte *et al.*, Evidence for eccentricity in the population of binary black holes observed by LIGO-Virgo-KAGRA (2024), [arXiv:2404.14286 \[gr-qc\]](https://arxiv.org/abs/2404.14286).

[52] G. Morras, G. Pratten, and P. Schmidt, Orbital eccentricity in a neutron star - black hole binary (2025), [arXiv:2503.15393 \[astro-ph.HE\]](https://arxiv.org/abs/2503.15393).

[53] A. Buonanno, B. Iyer, E. Ochsner, Y. Pan, and B. S. Sathyaprakash, Comparison of post-Newtonian templates for compact binary inspiral signals in gravitational-wave detectors, *Phys. Rev. D* **80**, 084043 (2009), [arXiv:0907.0700 \[gr-qc\]](https://arxiv.org/abs/0907.0700).

[54] B. Moore, M. Favata, K. G. Arun, and C. K. Mishra, Gravitational-wave phasing for low-eccentricity inspiralling compact binaries to 3PN order, *Phys. Rev. D* **93**, 124061 (2016), [arXiv:1605.00304 \[gr-qc\]](https://arxiv.org/abs/1605.00304).

[55] B. P. Abbott *et al.* (LIGO Scientific, Virgo), GW150914: First results from the search for binary black hole coalescence with Advanced LIGO, *Phys. Rev. D* **93**, 122003 (2016), [arXiv:1602.03839 \[gr-qc\]](https://arxiv.org/abs/1602.03839).

[56] A. Viets *et al.*, Reconstructing the calibrated strain signal in the Advanced LIGO detectors, *Class. Quant. Grav.* **35**, 095015 (2018), [arXiv:1710.09973 \[astro-ph.IM\]](https://arxiv.org/abs/1710.09973).

[57] A. G. Abac *et al.* (LIGO Scientific, VIRGO, KAGRA), GWTC-4.0: Methods for Identifying and Characterizing Gravitational-wave Transients (2025), [arXiv:2508.18081 \[gr-qc\]](https://arxiv.org/abs/2508.18081).

[58] G. Pratten, S. Husa, C. Garcia-Quiros, M. Colleoni, A. Ramos-Buades, H. Estelles, and R. Jaume, Setting the cornerstone for a family of models for gravitational waves from compact binaries: The dominant harmonic for nonprecessing quasicircular black holes, *Phys. Rev. D* **102**, 064001 (2020), [arXiv:2001.11412 \[gr-qc\]](https://arxiv.org/abs/2001.11412).

[59] L. Pompili *et al.*, Laying the foundation of the effective-one-body waveform models SEOBNRv5: Improved accuracy and efficiency for spinning nonprecessing binary black holes, *Phys. Rev. D* **108**, 124035 (2023), [arXiv:2303.18039 \[gr-qc\]](https://arxiv.org/abs/2303.18039).

[60] A. Buchholz, N. Chopin, and P. E. Jacob, Adaptive tuning of hamiltonian monte carlo within sequential monte carlo, *Bayesian Analysis* **16**, 745 (2021).

[61] T. Le Thu Nguyen, F. Septier, G. W. Peters, and Y. Delignon, Improving smc sampler estimate by recycling all past simulated particles, in *2014 IEEE Workshop on Statistical Signal Processing (SSP)* (2014) pp. 117–120.

[62] M. Karamanis and U. Seljak, Persistent sampling: Enhancing the efficiency of sequential monte carlo, *Statistics and Computing* **35**, 1 (2025).

[63] M. M. Graham and A. J. Storkey, Continuously tempered Hamiltonian Monte Carlo, [arXiv e-prints](https://arxiv.org/abs/1704.03338), [arXiv:1704.03338 \[stat.CO\]](https://arxiv.org/abs/1704.03338).

[64] A. H. Nitz, Robust, rapid, and simple gravitational-wave parameter estimation, *Phys. Rev. D* **112**, 023032 (2025), [arXiv:2410.05190 \[astro-ph.IM\]](https://arxiv.org/abs/2410.05190).

[65] G. Cabourn Davies *et al.*, Premerger observation and characterization of massive black hole binaries, *Phys. Rev. D* **111**, 043045 (2025), [arXiv:2411.07020 \[hep-ex\]](https://arxiv.org/abs/2411.07020).

[66] L. Gärtner, N. Hartmann, L. Heinrich, M. Horstmann, T. Kuhr, M. Reboud, S. Stefkova, and D. van Dyk, Constructing model-agnostic likelihoods, a method for the reinterpretation of particle physics results, *Eur. Phys. J. C* **84**, 693 (2024), [arXiv:2402.08417 \[hep-ph\]](https://arxiv.org/abs/2402.08417).

[67] R. Arjona, L. Espinosa-Portales, J. García-Bellido, and S. Nesseris, A GREAT model comparison against the cosmological constant, *Phys. Dark Univ.* **36**, 101029 (2022), [arXiv:2111.13083 \[astro-ph.CO\]](https://arxiv.org/abs/2111.13083).

[68] Z. G. Lane, A. Seifert, R. Ridden-Harper, and D. L. Wiltshire, Cosmological foundations revisited with Pantheon+, *Mon. Not. Roy. Astron. Soc.* **536**, 1752 (2025), [arXiv:2311.01438 \[astro-ph.CO\]](https://arxiv.org/abs/2311.01438).

[69] M. J. Williams, Accelerated Sequential Posterior Inference via Reuse for Gravitational-Wave Analyses - Data Release (2025).

[70] M. J. Williams, Accelerated Sequential Posterior Inference via Reuse for Gravitational-Wave Analyses - Code Release (2025).

[71] M. J. Williams, `aspire-inference`, Python Package Index (PyPI) (2025).

[72] M. J. Williams, `aspire-bilby`, Python Package Index (PyPI) (2025).

[73] M. J. Williams, `aspire-gw`, Python Package Index (PyPI) (2025).

[74] R. Abbott *et al.* (LIGO Scientific, Virgo), Open data from the first and second observing runs of Advanced LIGO and Advanced Virgo, *SoftwareX* **13**, 100658 (2021), [arXiv:1912.11716 \[gr-qc\]](https://arxiv.org/abs/1912.11716).

[75] C. for Python Data API Standards, array-api-compat, <https://pypi.org/project/array-api-compat/> (2025).

[76] G. Ashton *et al.*, BILBY: A user-friendly Bayesian inference library for gravitational-wave astronomy, *Astrophys. J. Suppl.* **241**, 27 (2019), [arXiv:1811.02042 \[astro-ph.IM\]](https://arxiv.org/abs/1811.02042).

[77] C. Talbot, G. Ashton, M. Hübner, M. Pitkin, plasky, asb5468, M. J. Williams, R. Smith, A. Vijaykumar, SMorisaki, J. Veitch, N. Sarin, D. Macleod, D. Williams, MarcArene, JasperMartins, C. P. L. Berry, V. Raymond, Ceciliogq, I. Markin, D. Keitel, AlexandreGoettel, L. Pompili, M. Wright, oliviawilk, noahewolfe, jacobgolomb, S. Wu, R. Udall, and M. Pürer, `bilby-dev/bilby: v2.5.2` (2025).

[78] D. Foreman-Mackey, corner.py: Scatterplot matrices in python, *The Journal of Open Source Software* **1**, 24 (2016).

[79] J. S. Speagle, dynesty: a dynamic nested sampling package for estimating Bayesian posteriors and evi-

dences, *Mon. Not. Roy. Astron. Soc.* **493**, 3132 (2020), [arXiv:1904.02180](https://arxiv.org/abs/1904.02180) [astro-ph.IM].

[80] M. J. Williams, [mj-will/gwflow](https://github.com/mj-will/gwflow): v0.1.0a1 (2025).

[81] LIGO Scientific Collaboration, **LIGO Algorithm Library - LALSuite**, free software (GPL) (2018).

[82] K. Wette, SWIGLAL: Python and Octave interfaces to the LALSuite gravitational-wave data analysis libraries, *SoftwareX* **12**, 100634 (2020).

[83] J. D. Hunter, Matplotlib: A 2d graphics environment, *Computing in Science & Engineering* **9**, 90 (2007).

[84] M. J. Williams, [mj-will/minipcn](https://github.com/mj-will/minipcn) (2025).

[85] C. R. Harris, K. J. Millman, S. J. van der Walt, R. Gommers, P. Virtanen, D. Cournapeau, E. Wieser, J. Taylor, S. Berg, N. J. Smith, R. Kern, M. Picus, S. Hoyer, M. H. van Kerkwijk, M. Brett, A. Haldane, J. F. del Río, M. Wiebe, P. Peterson, P. Gérard-Marchant, K. Sheppard, T. Reddy, W. Weckesser, H. Abbasi, C. Gohlke, and T. E. Oliphant, Array programming with NumPy, *Nature* **585**, 357 (2020).

[86] C. Hoy and V. Raymond, PESummary: the code agnostic Parameter Estimation Summary page builder, *SoftwareX* **15**, 100765 (2021), [arXiv:2006.06639](https://arxiv.org/abs/2006.06639) [astro-ph.IM].

[87] A. Paszke *et al.*, PyTorch: An Imperative Style, High-Performance Deep Learning Library (2019), [arXiv:1912.01703](https://arxiv.org/abs/1912.01703) [cs.LG].

[88] Wes McKinney, Data Structures for Statistical Computing in Python, in *Proceedings of the 9th Python in Science Conference*, edited by Stéfan van der Walt and Jarrod Millman (2010) pp. 56 – 61.

[89] P. Virtanen, R. Gommers, T. E. Oliphant, M. Haberland, T. Reddy, D. Cournapeau, E. Burovski, P. Peterson, W. Weckesser, J. Bright, S. J. van der Walt, M. Brett, J. Wilson, K. J. Millman, N. Mayorov, A. R. J. Nelson, E. Jones, R. Kern, E. Larson, C. J. Carey, I. Polat, Y. Feng, E. W. Moore, J. VanderPlas, D. Laxalde, J. Perktold, R. Cimrman, I. Henriksen, E. A. Quintero, C. R. Harris, A. M. Archibald, A. H. Ribeiro, F. Pedregosa, P. van Mulbregt, and SciPy 1.0 Contributors, SciPy 1.0: Fundamental Algorithms for Scientific Computing in Python, *Nature Methods* **17**, 261 (2020).

[90] M. L. Waskom, seaborn: statistical data visualization, *Journal of Open Source Software* **6**, 3021 (2021).

[91] F. Rozet *et al.*, Zuko: Normalizing flows in pytorch (2024).

[92] G. Papamakarios, T. Pavlakou, and I. Murray, Masked Autoregressive Flow for Density Estimation (2017), [arXiv:1705.07057](https://arxiv.org/abs/1705.07057) [stat.ML].

[93] D. P. Kingma and J. Ba, Adam: A Method for Stochastic Optimization (2014) [arXiv:1412.6980](https://arxiv.org/abs/1412.6980) [cs.LG].

[94] I. Loshchilov and F. Hutter, SGDR: Stochastic Gradient Descent with Warm Restarts (2016), [arXiv:1608.03983](https://arxiv.org/abs/1608.03983) [cs.LG].

[95] M. Karamanis, D. Nabergoj, F. Beutler, J. A. Peacock, and U. Seljak, pocoMC: A Python package for accelerated Bayesian inference in astronomy and cosmology, *J. Open Source Softw.* **7**, 4634 (2022), [arXiv:2207.05660](https://arxiv.org/abs/2207.05660) [astro-ph.IM].

[96] R. D. P. Grumitt, M. Karamanis, and U. Seljak, Sequential Kalman tuning of the t-preconditioned Crank-Nicolson algorithm: efficient, adaptive and gradient-free inference for Bayesian inverse problems, *Inverse Problems* **40**, 125023 (2024), [arXiv:2407.07781](https://arxiv.org/abs/2407.07781) [stat.CO].

[97] M. J. Williams, [mj-will/aspire-gw](https://github.com/mj-will/aspire-gw): v0.1.0a1 (2025).

[98] B. P. Abbott *et al.* (KAGRA, LIGO Scientific, Virgo), Prospects for observing and localizing gravitational-wave transients with Advanced LIGO, Advanced Virgo and KAGRA, *Living Rev. Rel.* **19**, 1 (2016), [arXiv:1304.0670](https://arxiv.org/abs/1304.0670) [gr-qc].

SUPPLEMENTAL MATERIAL

Implementation details

The complete implementation of ASPIRE combines the two steps described in the main text. The algorithm takes as input an initial set of posterior samples, together with a prior and likelihood for a new model. A normalizing flow is first trained on the initial samples to approximate their density; in this work we use masked autoregressive flows [92] as implemented in `zuko` [91]. Training is performed using the Adam optimizer [93] with an initial learning rate of 0.001, decayed by cosine annealing [94], and a batch size of 500. The trained flow serves as the proposal distribution $q(\theta)$ in the generalized SMC eq. (2). We employ the standard SMC framework with adaptive temperature selection following [95], which makes the method robust to the choice of initial samples. Particle diversification is performed with a t -preconditioned Crank–Nicolson MCMC kernel [96], using the lightweight `minipcn` implementation [84]. We implement this in `aspire` [40] and also provide an interface for the `bilby` inference library [76, 77] through the companion package `aspire-bilby`, which facilitates the direct application of ASPIRE in gravitational-wave analyses.

For the reanalysis of GW150914, we employ a custom normalizing-flow architecture designed to handle the additional calibration parameters. Since the marginal posteriors for the 40 calibration parameters are approximately Gaussian and weakly correlated, we model them with a multivariate Gaussian with mean and diagonal covariance matrix, both learned during training of the normalizing flow. We begin with a 50-epoch pre-training stage in which only the mean and covariance are optimized. This is implemented in `gwflow` [80] which builds on `zuko` and interfaces with `aspire` via the companion package `aspire-gw` [97].

Analysis details

All injection studies were performed with simulated signals in a three-detector network at O4 design sensitivity [98]. Analyses were carried out using `bilby`. Baseline analyses used `dynesty`, as implemented in `bilby`, with the settings described in [57]. Data for the probability–probability tests were simulated an 8-second duration, coloured Gaussian noise at O4 design sensitivity and `IMRPhenomXPHM` using the priors described in [22].

In cases where certain parameters in one model are incompatible with those in another, we replace the posterior samples for the incompatible parameters with draws from the prior. For example, when transitioning between `IMRPhenomXPHM` and `IMRPhenomX04a`, we replace the samples for the polarization angle and phase of coalescence. For highly asymmetric mass ratios, we also replace the samples for the chirp mass and mass ratio. When introducing spin precession, the aligned-spin samples are replaced, and when adding eccentricity, we replace both mass and spin samples, since `TaylorF2` finds the signal to be highly spinning.

All analyses were performed using `bilby` and `bilby-pipe`. Analyses of simulated data used 16 CPU cores for parallelization while analyses of real data used 32.